THE SLOAN DIGITAL SKY SURVEY REVERBERATION MAPPING PROJECT: Hα AND Hβ REVERBERATION MEASUREMENTS FROM FIRST-YEAR SPECTROSCOPY AND PHOTOMETRY

C. J. Grier[1,2], J. R. Trump[1,3], Yue Shen[4,5,*], Keith Horne[6], Karen Kinemuchi[7], Ian D. McGreer[8], D. A. Starkey[6], W. N. Brandt[1,2,9], P. B. Hall[10], C. S. Kochanek[11,12], Yuguang Chen[13], K. D. Denney[11, 12, 14], Jenny E. Greene[15], L. C. Ho[16,17], Y. Homayouni[3], Jennifer I-Hsiu Li[4], Liuyi Pei[4], B. M. Peterson[11,12,18], P. Petitjean[19], D. P. Schneider[1,2], Mouyuan Sun[20], Yusura AlSayyad[15], Dmitry Bizyaev[7,21] Jonathan Brinkmann[7], Joel R. Brownstein[22], Kevin Bundy[23], K S. Dawson[22], Sarah Eftekharzadeh[24], J. G. Fernandez-Trincado[25], Yang Gao[26,27], Timothy A. Hutchinson[22], Siyao Jia[28], Linhua Jiang[16], Daniel Oravetz[7], Kaike Pan[7], Isabelle Paris[29], Kara A. Ponder[30], Christina Peters[31], Jesse Rogerson[32], Audrey Simmons[7], Robyn Smith[33], and Ran Wang[16]

Draft version November 10, 2017

We present reverberation mapping results from the first year of combined spectroscopic and photometric observations of the Sloan Digital Sky Survey Reverberation Mapping Project. We successfully recover reverberation time delays between the $g+i$- band emission and the broad Hβ emission line for a total of 44 quasars, and for the broad Hα emission line in 18 quasars. Time delays are computed using the `JAVELIN` and `CREAM` software and the traditional interpolated cross-correlation function (ICCF): Using well defined criteria, we report measurements of 32 Hβ and 13 Hα lags with `JAVELIN`, 42 Hβ and 17 Hα lags with `CREAM`, and 16 Hβ and 8 Hα lags with the ICCF. Lag values are generally consistent among the three methods, though we typically measure smaller uncertainties with `JAVELIN` and `CREAM` than with the ICCF, given the more physically motivated light curve interpolation and more robust statistical modeling of the former two methods. The median redshift of our Hβ-detected sample of quasars is 0.53, significantly higher than that of the previous reverberation-mapping sample. We find that in most objects, the time delay of the Hα emission is consistent with or slightly longer than that of Hβ. We measure black hole masses using our measured time delays and line widths for these quasars. These black hole mass measurements are mostly consistent with expectations based on the local $M_{\rm BH}$–σ_* relationship, and are also consistent with single-epoch black hole mass measurements. This work increases the current sample size of reverberation-mapped active galaxies by about two-thirds and represents the first large sample of reverberation mapping observations beyond the local universe ($z < 0.3$).

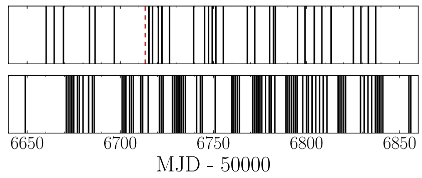

Fig. 2.— The observing cadence for the spectroscopic observations (top panel) and photometric observations (bottom panel). Each vertical black line represents an observed epoch. The seventh spectroscopic epoch, shown as a red dashed line, has much lower SNR and is frequently an outlier in the light curves, and so is excluded from our analysis.

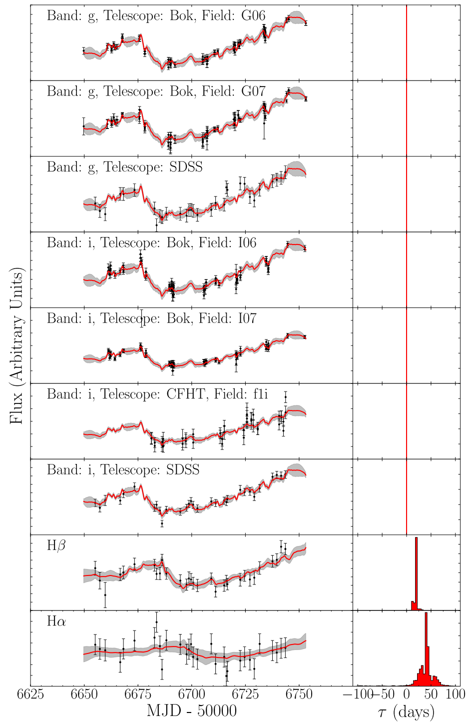

Fig. 3.— `CREAM` model fits to the light curves for SDSS J141625.71+535438.5 (RMID 272, $z = 0.263$) as a demonstration of the inter-calibration technique. Each left panel shows an individual pre-merged light curve (black points) with the `CREAM` model fit and uncertainties in red and gray, respectively. The right panels display the corresponding `CREAM`-calculated posterior distribution of observed-frame time lags calculated for each light curve's response function $\psi(\tau)$. The time lag between the photometric light curves and the synthetic spectroscopic light curves is fixed to zero in order to inter-calibrate the data.

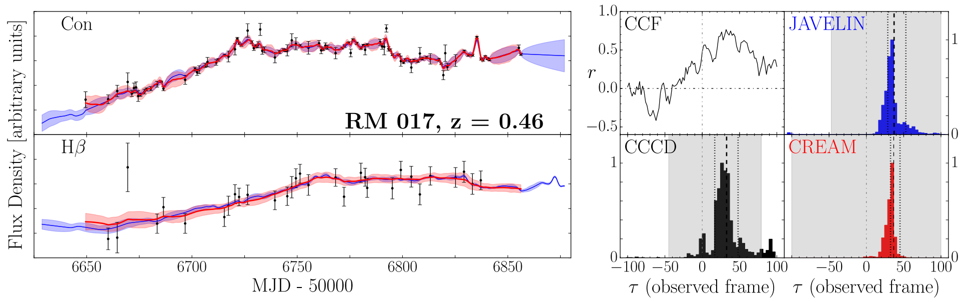

Fig. 6.— Light curves and models for the Hβ emission line analysis of SDSS J141324.28+530527.0 (RMID 017, $z = 0.456$). The continuum and Hβ light curves are presented in the top and bottom of the left panels. For display purposes, we show the weighted mean of all epochs observed within a single night. The `JAVELIN` model and the uncertainty envelope are given in blue, and the `CREAM` models and their uncertainties in red. The right four panels show the results of the time-series analysis. The top left panel shows the ICCF. The other three panels present the lag distributions for the three different methods, normalized to the tallest peak in the distribution. The bottom left panel shows the CCCD, the top right panel shows the `JAVELIN` posterior lag distribution, and the bottom right panel shows the `CREAM` posterior lag distribution. Black vertical dashed and dotted lines correspond to the measured observed-frame lag and its uncertainties. The gray dash-dotted vertical lines indicate a lag of zero to guide the eye, and the horizontal dash-dotted line in the CCF panel shows a cross-correlation coefficient r of 0. The gray shaded area covers the regions of the posteriors that were included in the measurements, as determined during the alias rejection procedure (see Section 3.2). Similar figures for each source are included in the online article.

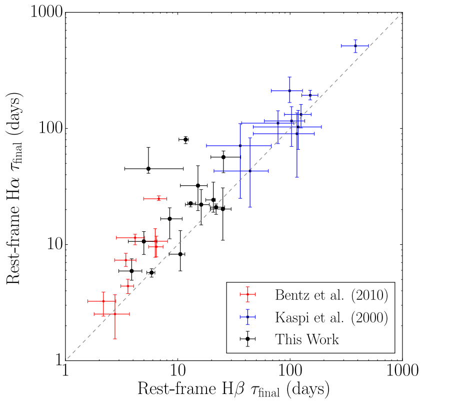

Fig. 10.— Hα vs. Hβ lag measurements for those objects where we detected significant lags for both emission lines (black filled circles). Red points represent measurements from Bentz et al. (2010), and blue squares represent measurements from Kaspi et al. (2000). The gray dashed line shows a ratio of one-to-one to guide the eye.

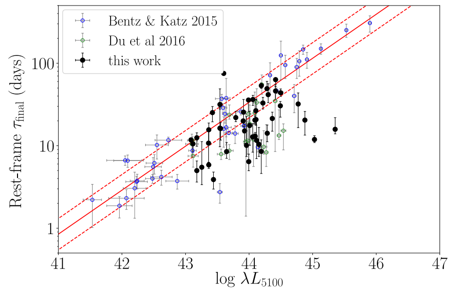

Fig. 11.— The Hβ $R-L$ relationship, with previous measurements in blue (Bentz & Katz 2015) and green (Du et al. 2016a) and our new measurements in black. The red solid and dashed lines show the best-fit relation and its measured scatter from Bentz et al. (2013). Many of the SDSS-RM and Du et al. (2016a) lags lie below the main $R-L$ relation: this may be (at least partly) due to selection effects from our limited monitoring cadence and duration, since our survey (and that of Du et al. 2016a) is not sensitive to long lags at high luminosities. The deviation may also be a physical effect associated with a different BLR size at high luminosities, or other quasar parameters that differ between the initial Bentz et al. (2013) dataset and the SDSS-RM and Du et al. (2016a) samples.

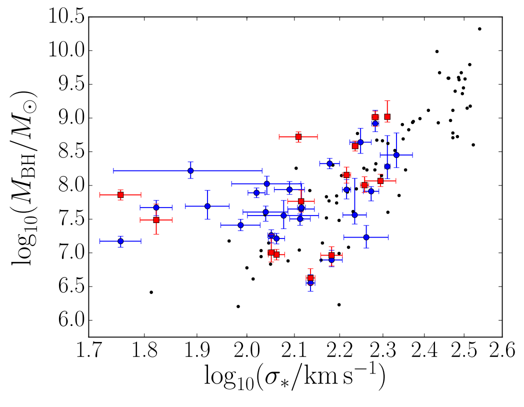

Fig. 14.— The $M_{\rm BH}$–σ_* relation with the sample of dynamical black hole masses from McConnell & Ma (2013) shown as black dots. Our new $M_{\rm BH}$ measurements made using the Hβ and Hα emission line time lags and line widths are represented by blue circles and red squares, respectively.

Revista Mexicana de Astronomía y Astrofísica, **00**, ??–?? (2007)

EMISSION LINE GALAXIES BEHIND THE PLANETARY NEBULA IC 5148: POTENTIAL FOR A SERENDIPITY SURVEY WITH ARCHIVAL DATA.

S. Kimeswenger[1,2] D. Barria[1] W. Kausch[2] D. S. Goldman[3]

Received June 5 2017; accepted October 5 2017

During the start of a survey program using FORS2 long slit spectroscopy on planetary nebulae (PN) and their haloes, we serendipitously discovered six background emission line galaxies (ELG) with redshifts of $z = 0.2057$, 0.3137, 0.37281, 0.4939, 0.7424 and 0.8668. Thus they clearly do not belong to a common cluster structure. We derived the major physical properties of the targets. Since the used long slit covers a sky area of only 570 arcsec^2 ($= 4.3 \times 10^{-5}$ square degrees), we discuss further potential of serendipitous discoveries in archival data, beside the deep systematic work of the ongoing and upcoming big surveys. We conclude that archival data provide a decent potential for extending the overall data on ELGs without any selection bias.